An augmented QCD phase portrait: Mapping quark-hadron deconfinement for hot, dense, rotating matter under magnetic field

Gaurav Mukherjee

BARC-HBNI, Mumbai

20 July, 2024

Outline of the talk

- Quark-gluon plasma, confinement-deconfinement, hadronization in **heavy-ions**
- Ubiquity of **rotation** and **magnetic fields** for different systems and scales
- Augment the planar phase diagram, zooming in on **quark-hadron transition**
- Thermodynamic effects, equation of state and phase transition
- Results: **augmented QCD phase diagram** in higher dimensional phase space
- Applicability and outlook: **Conclusions**

Particle accelerators to peer into the structure of matter

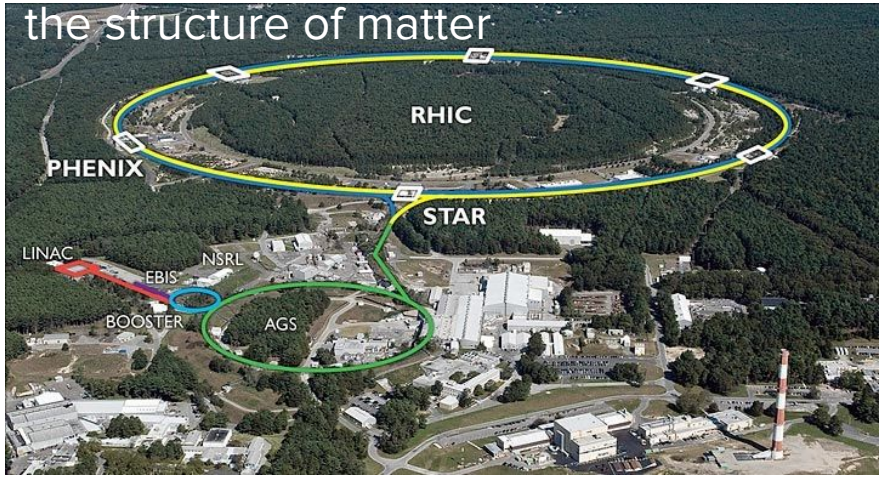

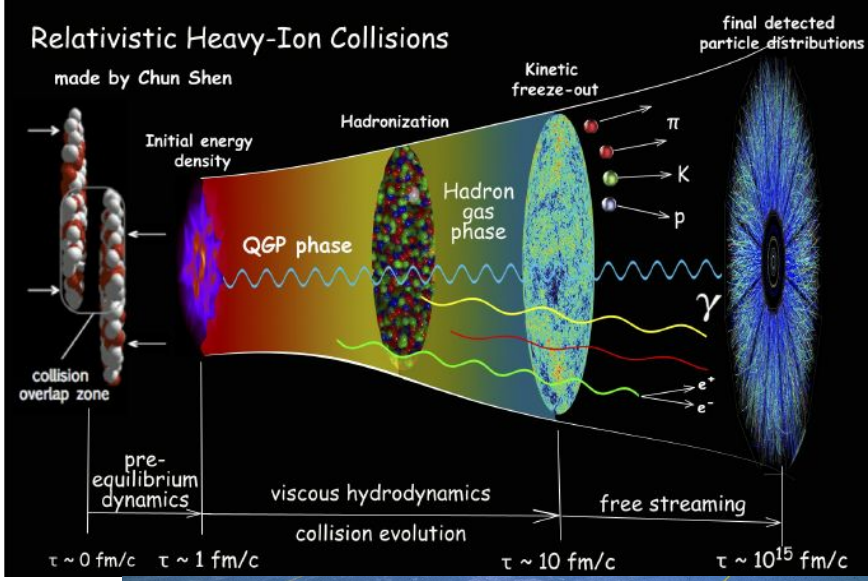

- Approximately one month of running time is dedicated to heavy-ions each year.

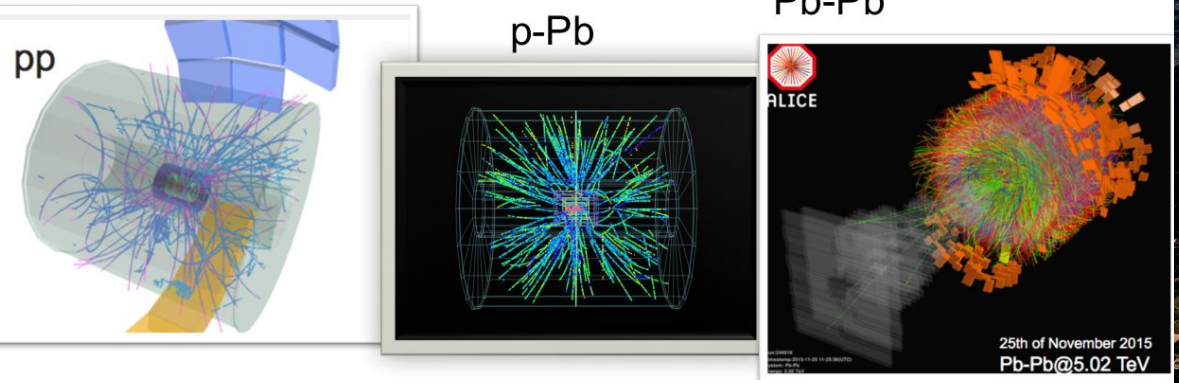

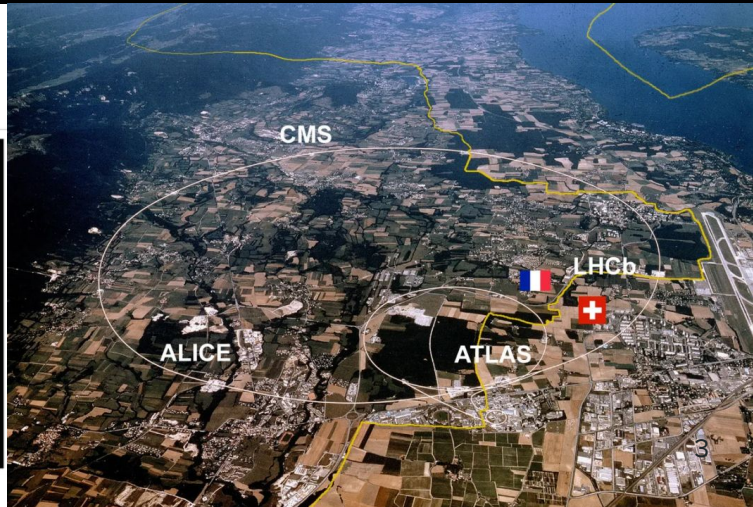

UltraRelativistic Heavy Ion Collisions (URHIC)

- Highly length-contracted heavy ion 'discs' collide to form fireball
- Nuclear matter transitions to QGP phase after collision

Depiction of an Off-central collision

Depiction of a Central collision

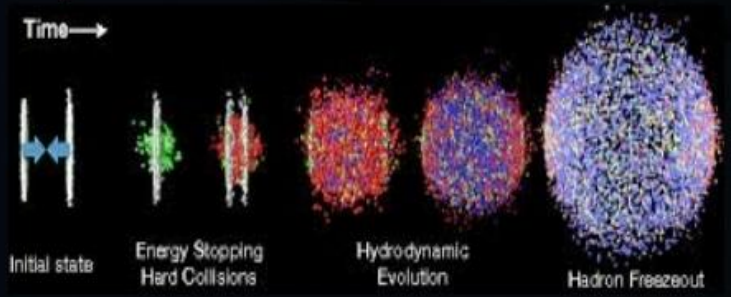

- System cools and expands
- Hadronization takes place due to confinement of the QCD color charges

Nature Physics | VOL 15 | OCTOBER 2019 | 1040–1045

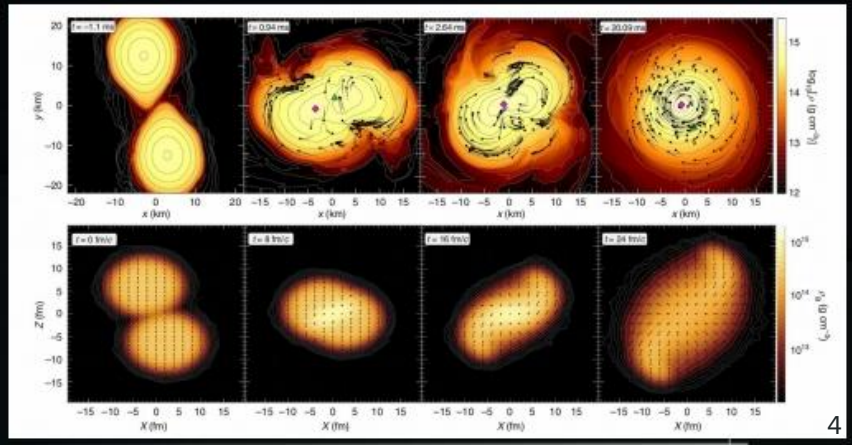

Heavy-ion collisions:
parallel global rotation and magnetic field for a generic non-central impact

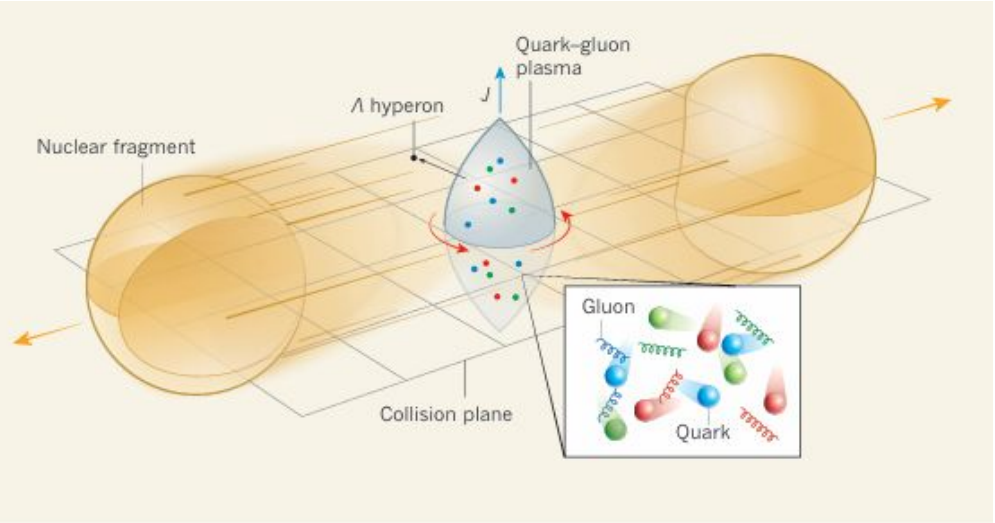

K. Hattori, Y. Yin / Nuclear Physics A 967 (2017) 768–771

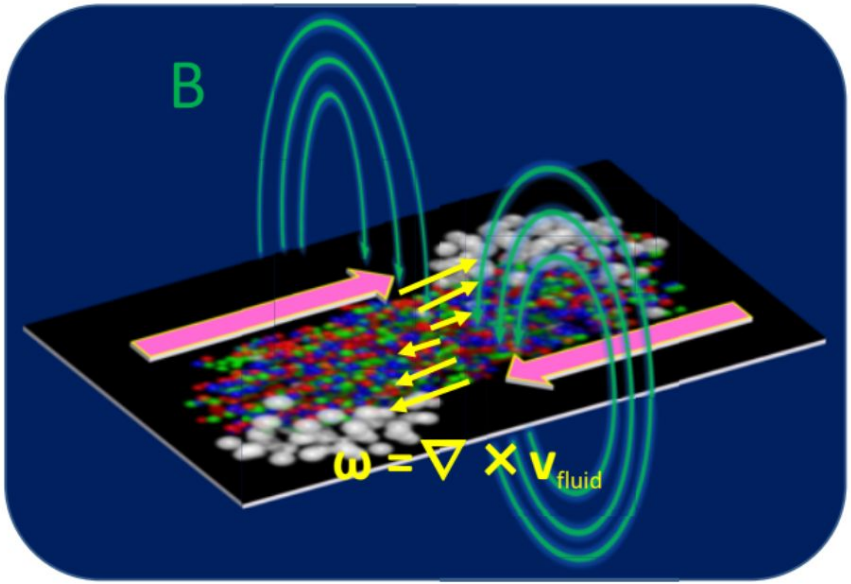

*In non-central collisions, QGP droplets perform a **spinning** ballet, and have a **magnetic** personality!*

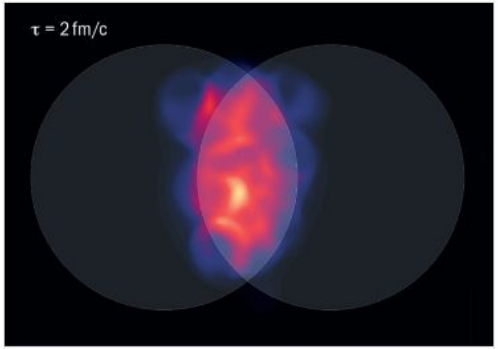

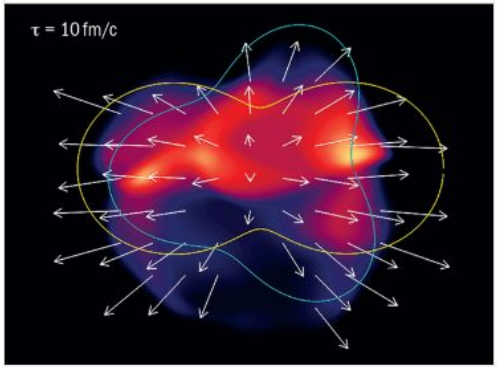

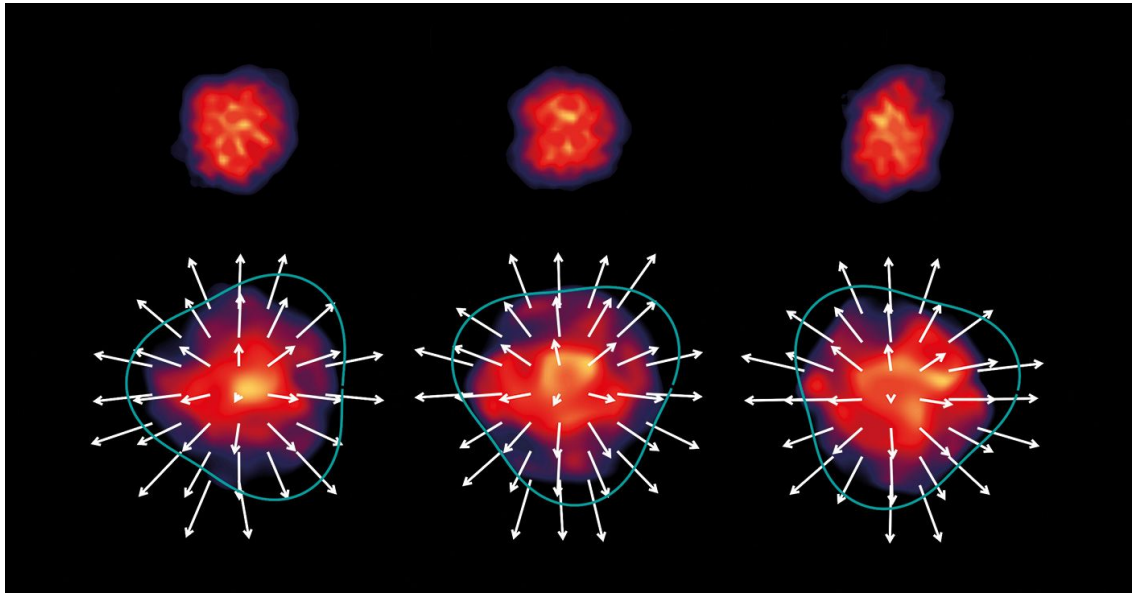

Noncentral collision An illustration of the evolving energy density of the QGP created in a noncentral collision. Pressure gradients act on the initial geometrical anisotropy to create a final velocity field (arrows), which may be decomposed into elliptic (yellow), triangular (teal) and higher order components. Hydrodynamic calculations were performed using the MUSIC software package. Credit: MUSIC arXiv:1209.6330

The QCD phase diagram

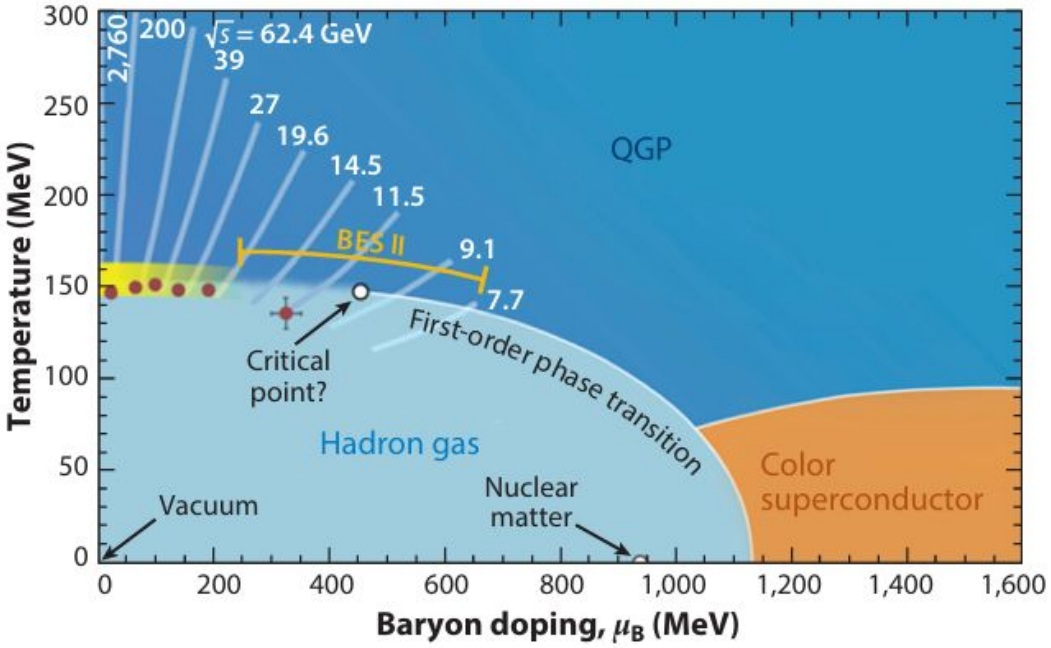

What systems traverse the different regions?

How can we probe the phase diagram?

Experimental handle: HICs and control parameters

QCD in astrophysics (neutron stars) and cosmology

Aim: a more comprehensive phase diagram

- Explore **QCD phase structure** in a

  (vorticity + magnetic field) augmented setting.

To get the full picture, where rotation parametrized by vorticity or angular velocity, and magnetic field may be non-zero simultaneously and included along with the temperature and net baryon density axes

Strategy to identify deconfinement

- A drastic rise in thermodynamic quantities like the entropy density at deconfinement
- Since this is of crossover type, we do not see a strict discontinuity or divergence but rather a sharp change within a narrow temperature window
- We choose a working condition for deconfinement along these lines [See: K. Fukushima, Phys. Lett. B 695 (2011) 387–391]
- Hadro-chemical freeze-out curve determined by universal freeze-out conditions can act as a close proxy for the deconfinement band region in the phase diagram, and this is most accurate in the small to medium baryon chemical potential range

- Dip in the squared speed of sound vs. temperature
- Unique temperatures where minima occur

HRG model under rotation

A quantum relativistic gas of all hadrons and resonances within a cylindrical boundary obeying the causality bound (due to the speed of light constraint)

$$p_i^{\pm} = \pm \frac{T}{8\pi^2} \sum_{\ell=-\infty}^{\infty} \int dk_r^2 \int dk_z \sum_{\nu=\ell}^{\ell+2S_i} J_\nu^2(k_r r) \times \log\left\{1 \pm \exp[-(\varepsilon_{\ell,i} - \mu_i)/T]\right\}$$

$$\varepsilon_{\ell,i} = \sqrt{k_r^2 + k_z^2 + m_i^2} - (\ell + S_i)\omega$$

Rotation induces an effective chemical potential

Causality bound: constraint from finite speed of light

$$R\,\omega \leq 1$$

$$\varepsilon \geq \frac{\xi_{\ell,1}}{R} \geq \xi_{\ell,1}\,\omega$$

Boundary condition important

$$\int dk_r^2 \quad \rightarrow \quad \int_{(\Lambda_\ell^{\mathrm{IR}})^2} dk_r^2$$

$$\Lambda_\ell^{\mathrm{IR}} = \xi_{\ell,1}\omega$$

Y.Fujimoto, K.Fukushima, Y.Hidaka, Physics Letters B 816 (2021) 136184

Deconfining phase boundary under rotation

Y. Fujimoto, K. Fukushima and Y. Hidaka

Physics Letters B 816 (2021) 136184

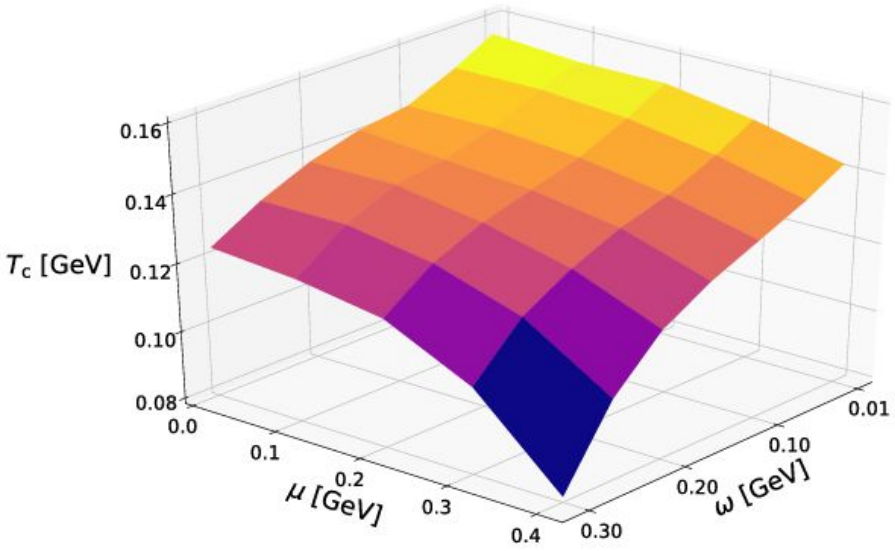

Fig. 2. Deconfinement transition surface as a function of the baryon chemical potential μ and the angular velocity ω.

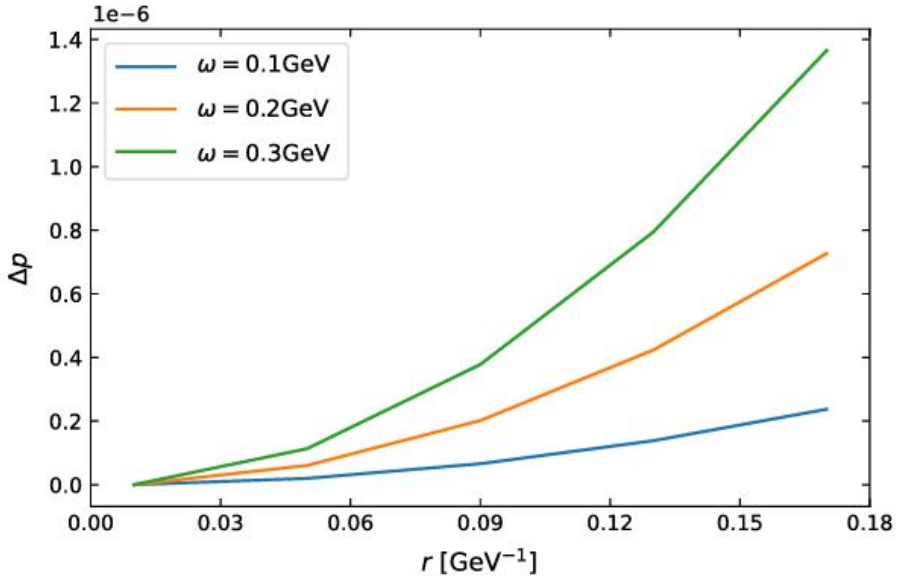

Fig. 3. Δp as a function of r for three different values of ω.

Inhomogeneity from centrifugation

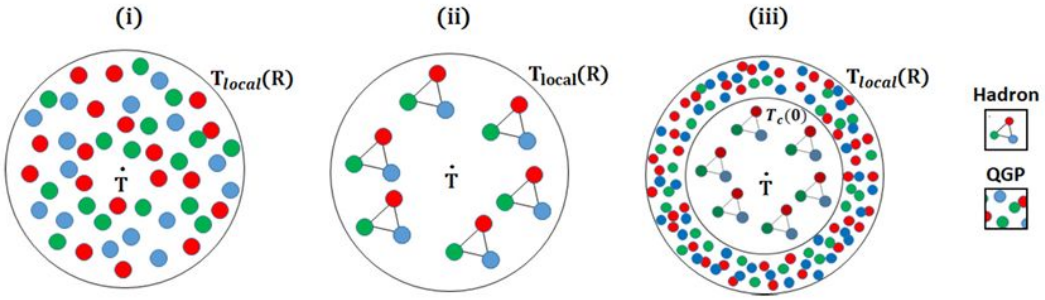

Fig. 2. Configurations of rotating QCD matter in the region $0 < \rho < R$. i) QGP without phase transition for $T > T_c(0)$. ii) Only hadronic matter for $T_c(0) > T_{local}(R)$. iii) Phase transition at ρ_c when $T_{\rm local}(\rho_c) = T_c(0)$.

Braga et al., Physics Letters B 848 (2024) 138330

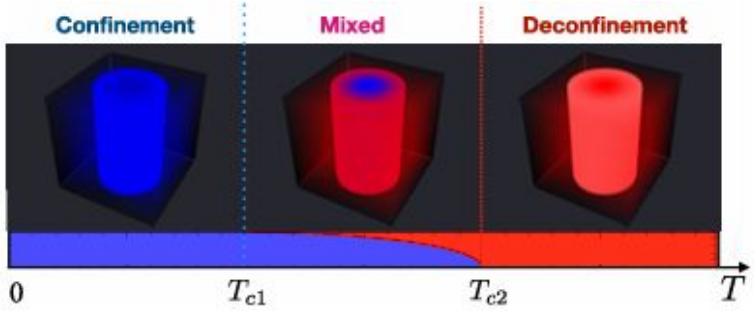

FIG. 7. Illustration of the confining, mixed, and deconfining phases of the uniformly rotating system at finite temperature.

Spatial inhomogeneity in the confined and deconfined phases from rotation even in a continuous crossover transition may manifest

Chernodub, Physical Review D 103, 054027 (2021)

HRG model under magnetic field

A quantum relativistic gas of all hadrons and resonances embedded in a uniform, static magnetic field

$$f_{\rm c}(s) = \mp \sum_{s_z} \sum_{k=0}^{\infty} \frac{qB}{2\pi} \int \frac{{\rm d}p_z}{2\pi} \left(\frac{E(p_z,k,s_z)}{2} + T \log(1 \pm e^{-E(p_z,k,s_z)/T}) \right)$$

Landau levels

$$E(p_z,k,s_z) = \sqrt{p_z^2 + m^2 + 2qB\,(k+1/2-s_z)},$$

$$f_{\rm n}(s) = \mp \sum_{s_z} \int \frac{{\rm d}^3\mathbf{p}}{(2\pi)^3} \left(\frac{E_0(\mathbf{p})}{2} + T \log(1 \pm e^{-E_0(\mathbf{p})/T}) \right)$$

$$E_0(\mathbf{p}) = \sqrt{\mathbf{p}^2 + m^2}.$$

Vacuum part needs renormalization

$$f^{\rm vac}(s) = f(s)|_{T=0}\,, \qquad f^{\rm therm}(s) = f(s) - f^{\rm vac}(s)$$

Endrodi, JHEP04(2013)023

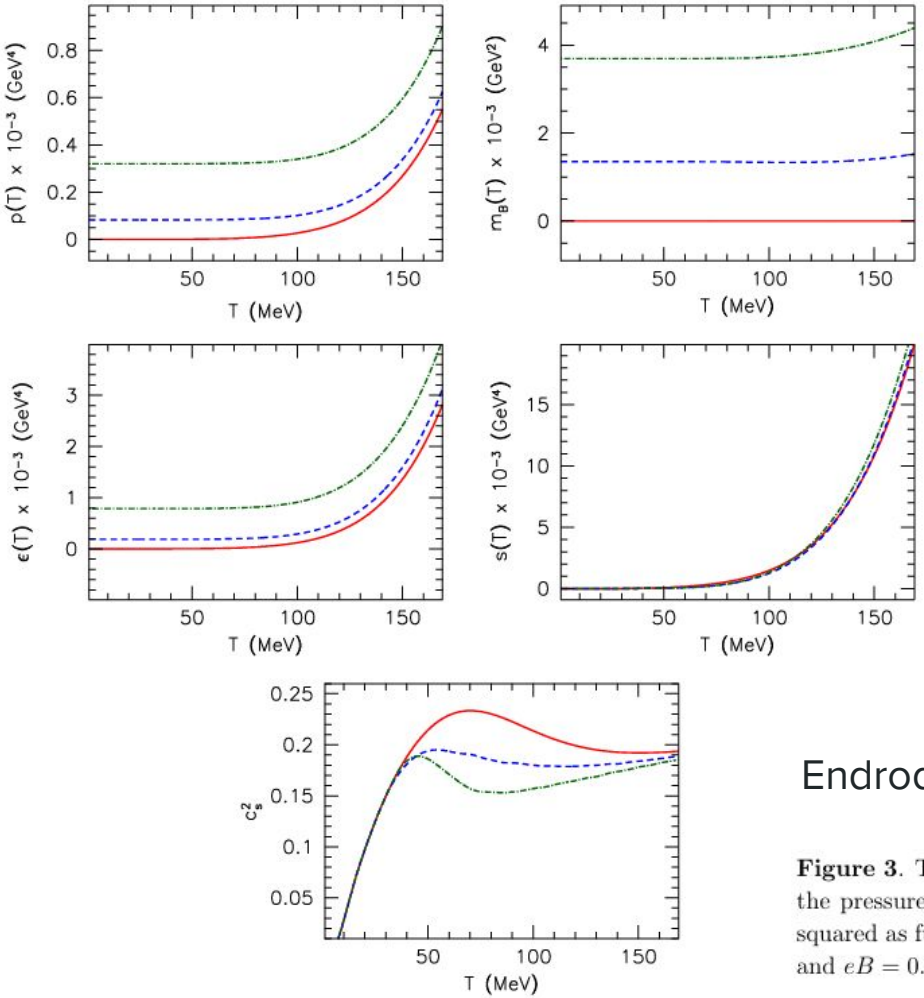

To evade divergences and renormalization calculations we can choose the entropy density and squared speed of sound to impose suitable criteria that yield the deconfinement temperature

Caveat: instability for the spin 3/2 channel

Endrodi, JHEP04(2013)023

Figure 3. The equation of state in the HRG model. Shown are (from left to right and downwards) the pressure, the magnetization, the energy density, the entropy density and the speed of sound squared as functions of the temperature, for $eB = 0$ (solid red lines), $eB = 0.2$ GeV^2 (dashed blue) and $eB = 0.3$ GeV^2 (dot-dashed green).

HRG model under parallel rotation and magnetic field

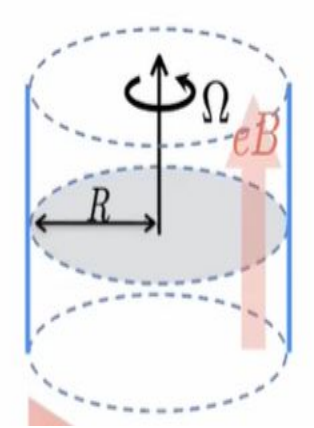

Rotation : transverse size finite

Magnetic field : Landau quantization when boundary effects can be neglected, that is, when the magnetic length is much smaller than the system size

These constraints restrict the validity of the model results to certain regimes of the various parameters.

Fortunately physical systems of interest are expected to lie in this parameter space

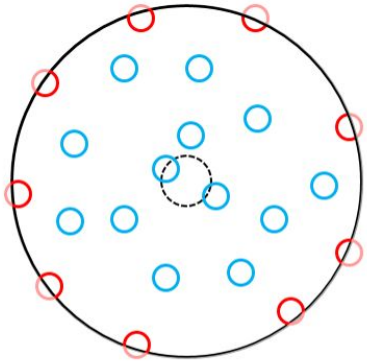

$B_1 >$

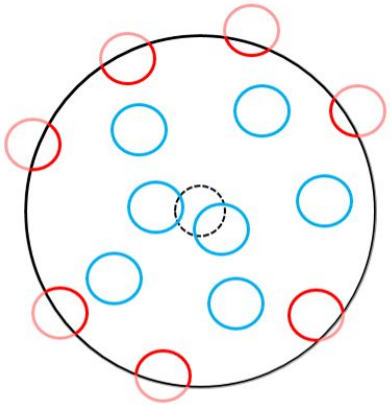

$B_2 >$

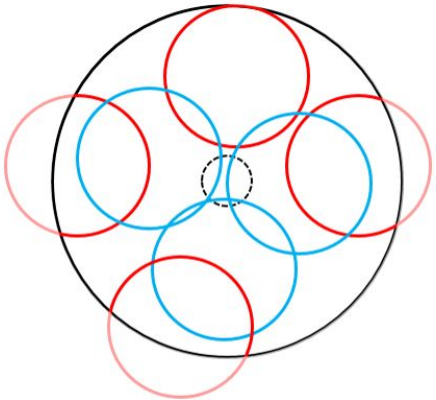

$B_3 >$

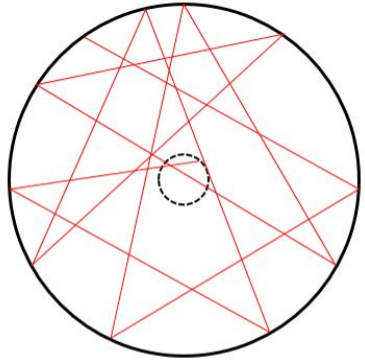

$B = 0$

$$1/\sqrt{|Q\,B|} \ll R \leqslant 1/\omega.$$

c = 1

Causality mandates boundary to maintain
Tangential velocity < Speed of light
Bulk physics unaffected by boundary for
Strong enough magnetic fields
As magnetic length, l_B << system size

Boundary conditions make finite-size effects important only when $l_{\text{system}} \lesssim l_B$ which corresponds to a very narrow sliver ($0 < eB \lesssim 0.0064$ GeV^2 for $l_B \sim l_{\text{system}} = 12.5$ GeV^{-1} or 2.5 fm) in the phase space that we will investigate. Also, these distortions occur due to the so-called edge states and become essentially irrelevant in the deep interior, i.e., $r \ll R$, of the system where only the bulk states dominate . Depicted above, schematically

Statistical Hadronization Model, aka Hadron Resonance Gas model in the presence of global vorticity & external in-medium magnetic field

$$1/\sqrt{|Q\,B|} \ll R \leqslant 1/\omega.$$

Landau quantization and Causality bound, Thermodynamic potential or free energy density

$$f_{i,c}^{b/m} = \mp \frac{T}{\pi R^2} \int \frac{dp_z}{2\pi} \sum_{n=0}^{\infty} \sum_{l=-n}^{N-n} \sum_{s_z=-s_i}^{s_i} \ln(1 \pm e^{-(\varepsilon_{i,c} - q_i\omega(l+s_z) - \mu_i)/T}), \tag{10}$$

where the dispersion relation contains the Landau levels

$$\varepsilon_{i,c} = \sqrt{p_z^2 + m_i^2 + |Q_i B|(2n - 2s_z + 1)}\ . \tag{11}$$

$$f_{i,n}^{b/m} = \mp \frac{T}{8\pi^2} \int\limits_{(\Lambda_l^{\rm IR})^2} dp_r^2 \int dp_z \sum_{l=-\infty}^{\infty} \sum_{\nu=l}^{l+2s_i} J_\nu^2(p_r r) \times \ln(1 \pm e^{-(\varepsilon_{i,n} - (l+s_i)\omega - \mu_i)/T}), \tag{12}$$

where the free part of the energy dispersion is given by

$$\varepsilon_{i,n} = \sqrt{p_r^2 + p_z^2 + m_i^2}\ . \tag{13}$$

Landau quantized spectra and the Dimensional reduction of Phase space

$$p_\perp^2 = |QB|(2n + 1 - 2s_z),\ dp_x dp_y \to 2\pi p_\perp dp_\perp = 2\pi |QB| dn$$

$$\int \frac{dp_x dp_y}{(2\pi)^2} \to \frac{|QB|}{2\pi} \sum_{n=0}^{\infty} \tag{1}$$

Landau degeneracy lifted due to Rotation

$$N = \frac{|QB|S}{2\pi},\quad S = \pi R^2$$

$$\int \frac{dp_x dp_y}{(2\pi)^2} \to \frac{1}{\pi R^2} \sum_{n=0}^{\infty} \sum_{l=-n}^{N-n} \tag{2}$$

Results: *μ, ω, eB, all finite*

Entropy density rises sharply and

Squared speed of sound dips rapidly

at deconfinement. These signal the

onset of deconfinement and can be

used as a proxy for the phase transition,

yielding the pseudo-critical or deconfinement

temperature.

Physics Letters B846(2023)138228

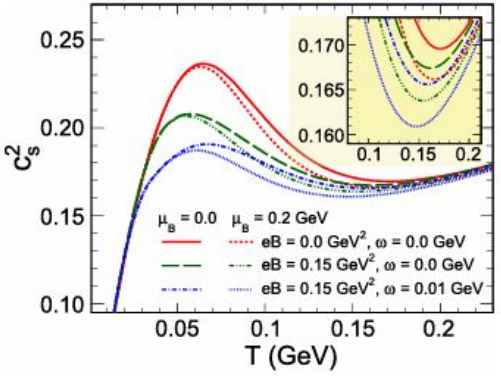

Fig. 1. The variation of the squared speed of sound as a function of temperature with a magnified view of the region where the minima occur in the inset.

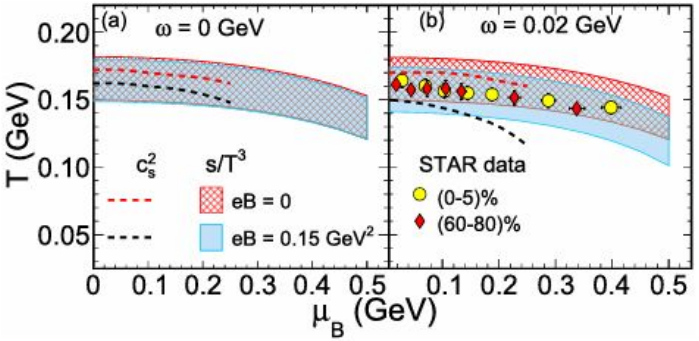

Fig. 2. QCD phase diagrams, T vs. μ_B for $eB = 0$ (red band or curve) and $eB = 0.15$ GeV^2 (blue band or curve) and (a) for $\omega = 0$ GeV and (b) for $\omega = 0.02$ GeV. The deconfinement transition zones depicted as (i) bands constrained by $s/T^3 = 4$ (lower edge) and 7 (upper edge), and (ii) curves obtained from the minima of χ_2^B vs. T as shown in Fig. 1.

Augmented QCD phase diagram

GM et al.,
Physics Letters B846(2023)138228

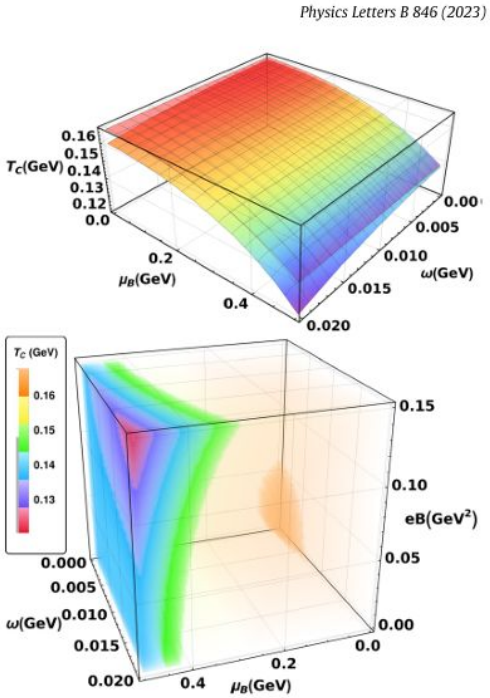

Fig. 3. (Top) Deconfinement transition surfaces showing $T_C(\mu_B,\ \omega)$ for $eB = 0$ (upper surface) and $eB = 0.15$ GeV^2 (lower surface). (Bottom) Augmented phase diagram showing $T_C(\mu_B,\ \omega,\ eB)$ as a color-coded density plot where the T_C-calibrated legend (left) provides reference for the different iso-T_C contour boundaries in the $\mu_B,\ \omega,\ eB$ space. Both plots obtained from rapid rise in entropy density at $s/T^3 = 5.5$.

Deconfinement temperature is lowered when baryon chemical potential, angular velocity and magnetic field take up finite values. These parameters seem to reinforce each other at high values where the decrease in the transition temperature is most prominent.

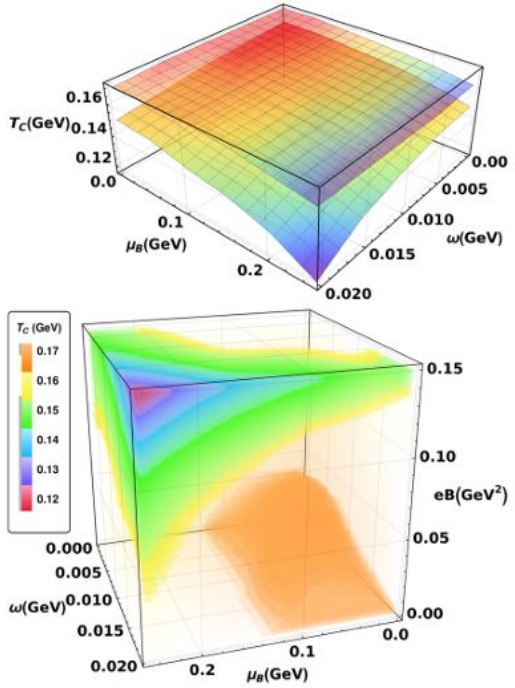

Fig. 4. (Top) Deconfinement transition surfaces showing $T_C(\mu_B,\ \omega)$ for $eB = 0$ (upper surface) and $eB = 0.15$ GeV^2 (lower surface). (Bottom) Augmented phase diagram showing $T_C(\mu_B,\ \omega,\ eB)$ as a color-coded density plot where the T_C-calibrated legend (left) provides reference for the different iso-T_C contour boundaries in the $\mu_B,\ \omega,\ eB$ space. Both obtained from the minima of the squared speed of sound.

Research findings, implications, scope for future works and conclusions

- Maximum drop in the deconfinement temperature is significant
- Thermal model (augmented) may be used as freeze-out probes and serve as

  thermometer, baryo-meter, anemometer, magnetometer
- Longer lifetime for the deconfined phase

- The cosmological QCD transition has been argued to have a uniquely important impact on both the formation of primordial black holes and the primordial gravitational wave background.
- Primordial vorticity and magnetic fields have also been hypothesized in the literature.
- It would be exciting to understand the gyromagnetic effects on these important exotic phenomena of the early universe.
- How the primordial cosmic fluid of the early universe materialized at the quark-hadron transition is an important fundamental question that becomes even more non-trivial when one adds into the mix vorticity and magnetic fields.
- Definitive answers are yet to come. It can be hoped that the insights and results found in the thesis will help pave the way.

Thank you

Acknowledgement:

Dipanwita Dutta, Dipak Kumar Mishra (Collaborators)

Thank you.

Mapping the Phases of quotidian (normal) & quantum (quark or QCD) matter

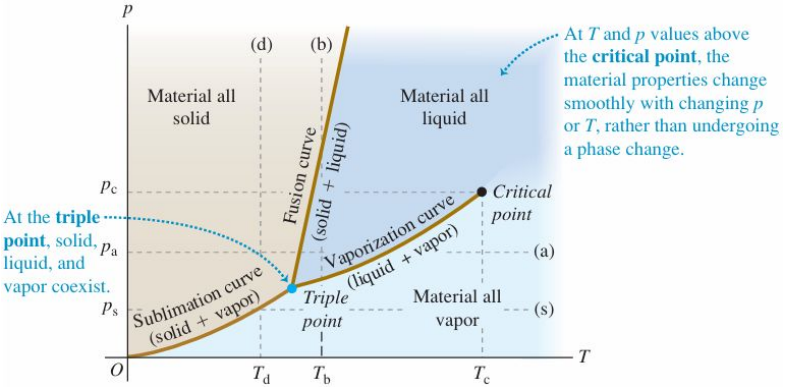

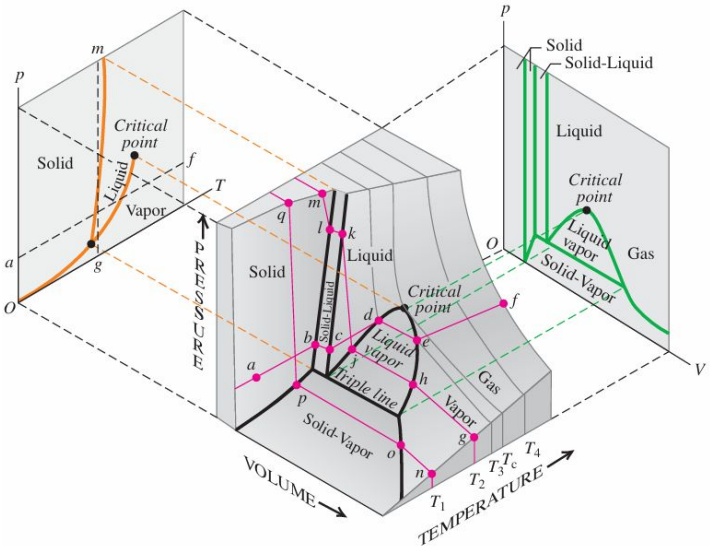

QCD phases: quark-gluon plasma (hot & dense), hadronic and nuclear matter

"Melting hadrons, boiling quarks"

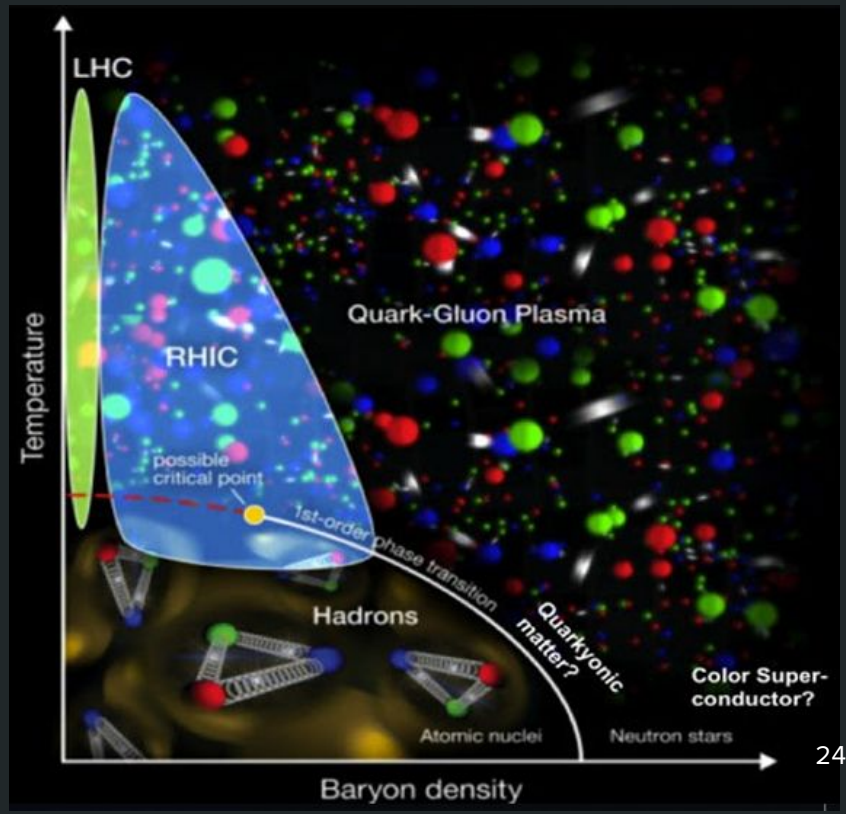

Transient nature of the magnetic field created by spectator nucleons

In this mechanism,

Spectator protons fly past the collision zone, creating very strong field in the overlap region where the fireball QGP droplet forms, but it is rapidly decaying

How long can the magnetic field last?

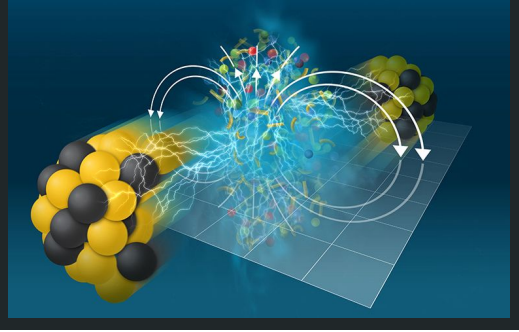

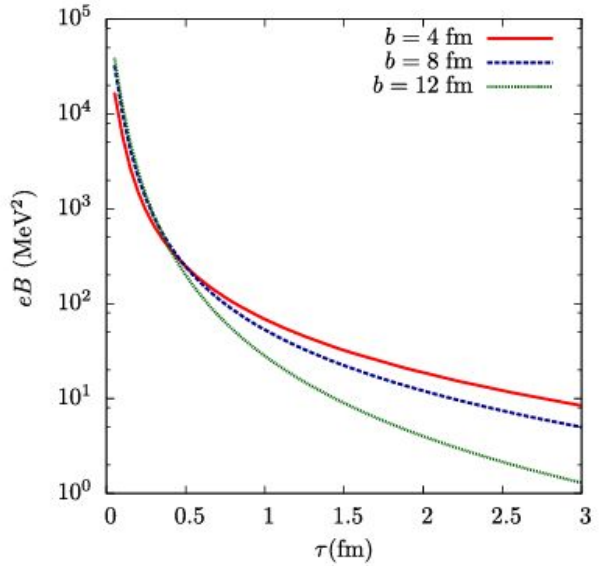

FIG. 1. Magnetic field as a function of proper time τ for three different values of the impact parameter b. From Kharzeev, McLerran, and Warringa, 2008.

Can other mechanisms extend the lifetime of the magnetic field?

Can we experimentally detect its signatures?

Yes!

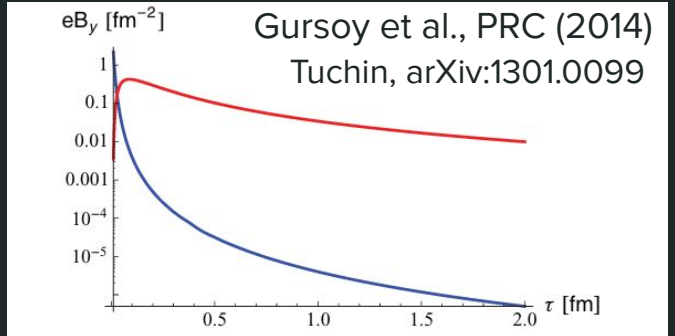

Gursoy et al., PRC (2014)
Tuchin, arXiv:1301.0099

FIG. 2. (Color online) Magnetic field B_y perpendicular to the reaction plane produced by the spectators in a heavy ion collision with impact parameter $b = 7$ fm at the LHC. The value of eB_y at the center of the collision, at $\eta = 0 = x_\perp$, is plotted as a function of τ. The blue curve shows how rapidly B_y at $\eta = 0 = x_\perp$ would decay as the spectators recede if there were no medium present, i.e., in vacuum with $\sigma = 0$. The presence of a conducting medium with $\sigma = 0.023$ fm^{-1} substantially delays the decay of B_y (red curve). At very early times before any medium has formed, when the blue curve is well above the red curve the blue curve is a better approximation.

Colossal Magnetic Field Detected in Nuclear Matter

February 23, 2024 • *Physics* 17, 31

Collisions of heavy ions briefly produced a magnetic field 10^{18} times stronger than Earth's, and it left observable effects.

Observation of the Electromagnetic Field Effect via Charge-Dependent Directed Flow in Heavy-Ion Collisions at the Relativistic Heavy Ion Collider

M. I. Abdulhamid *et al.* (STAR Collaboration)

Phys. Rev. X 14, 011028 (2024)

Published February 23, 2024

Statistical Hadronization Model aka Hadron Resonance Gas Model

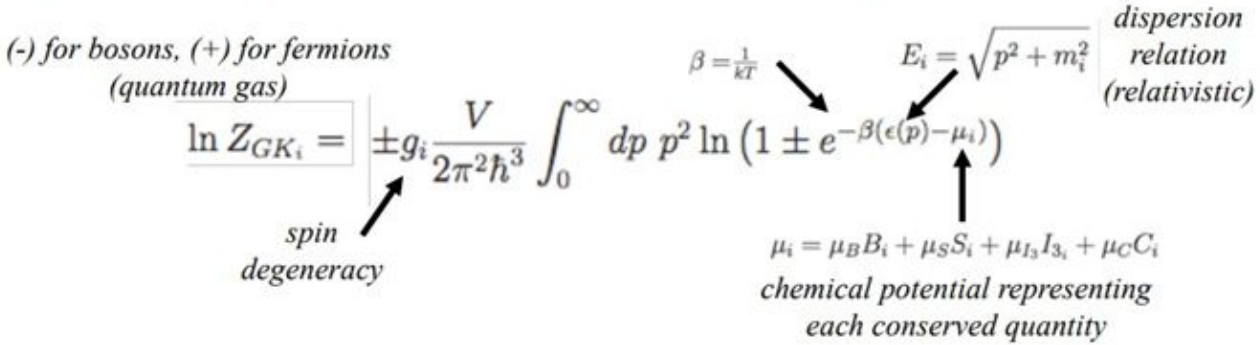

Only two free parameters are needed: **(T,μ_B)**. Volume cancels if particle ratios n_i/n_j are calculated. If yields are fitted, it acts as the third free parameter.

Relevant interactions are mediated via resonances

Non-interacting hadron resonance gas thus serves as a good approximation for an interacting hadron gas

Thermodynamics, Deconfinement and Freeze-out

HRG model provides theoretical access to the thermodynamics, confinement-deconfinement transition and also phenomenological to heavy-ion collisions via chemical freeze-out

Once the partition function is known, we can calculate all other thermodynamic quantities:

$$n = \frac{1}{V}\frac{\partial(T\ln Z)}{\partial\mu} \quad P = \frac{\partial(T\ln Z)}{\partial V} \quad s = \frac{1}{V}\frac{\partial(T\ln Z)}{\partial T}$$

Busza et al., Annu. Rev. Nucl. Part. Sci. 2018. 68:339–76

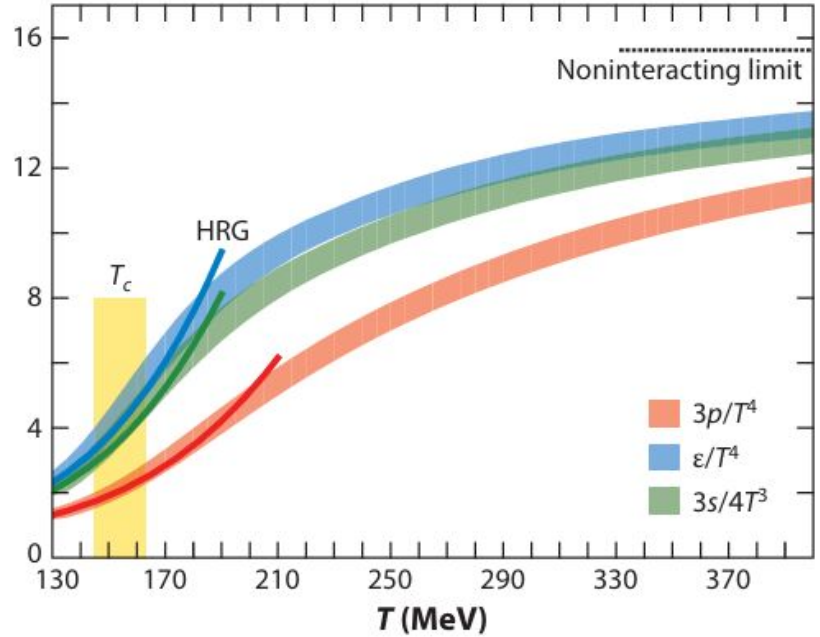

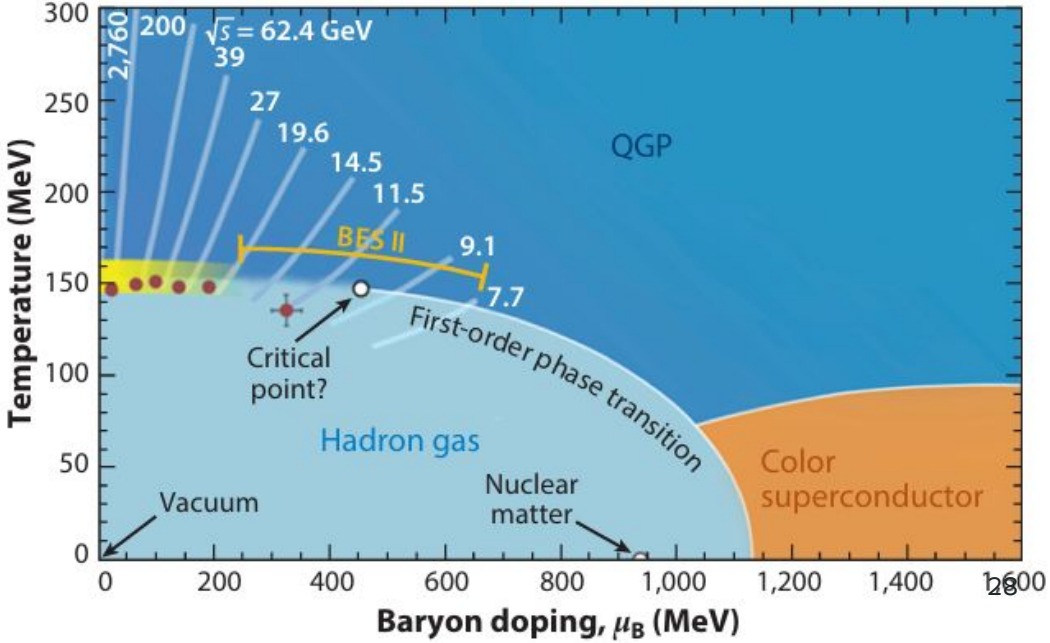

Strong magnetic field or weak rotation and finite size

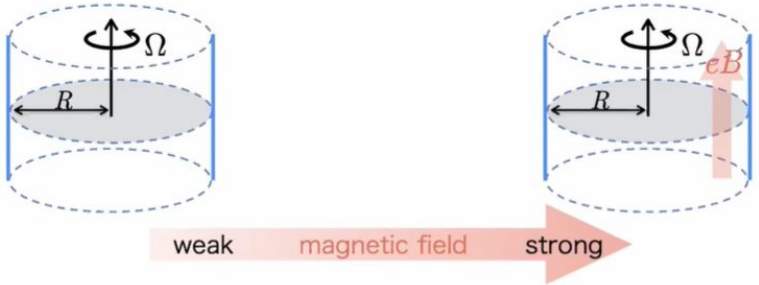

$$1/\sqrt{|Q\,B|} \ll R \lesssim 1/\omega.$$

Momentum Discretization

Bosons in a well

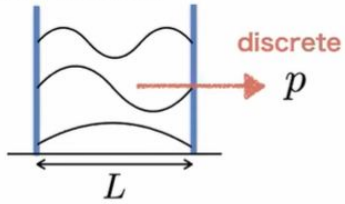

Dirichlet type

$$\sin(px)|_{x=L} = 0$$

$$\rightarrow \quad p = \frac{n\pi}{L} \geq \frac{\pi}{L}$$

IR gapped mode

Fermions in a cylinder

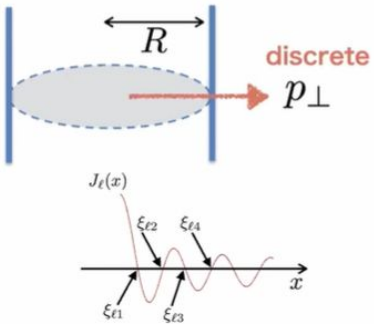

NO incoming current

$$\hat{e}_r \bar{\psi} \gamma^r \psi \Big|_{r=R} = 0$$

$$\rightarrow \quad p_\perp \mp \frac{\xi_{l,k}}{R} \geq \frac{\xi_{l,1}}{R}$$

IR gapped mode

$\xi_{l,k}$: the kth root of $J_l(x)$

The above inequalities may be satisfied by values relevant for a wide range of physical systems including HIC fireballs and perhaps even the early universe.

Thus this idealized model could be applicable in hitherto unexplored regimes.

Kazuya Mameda, Rotational effect versus finite-size effect
Chen et al., Phys. Rev. D 93 (10) (2016) 104052

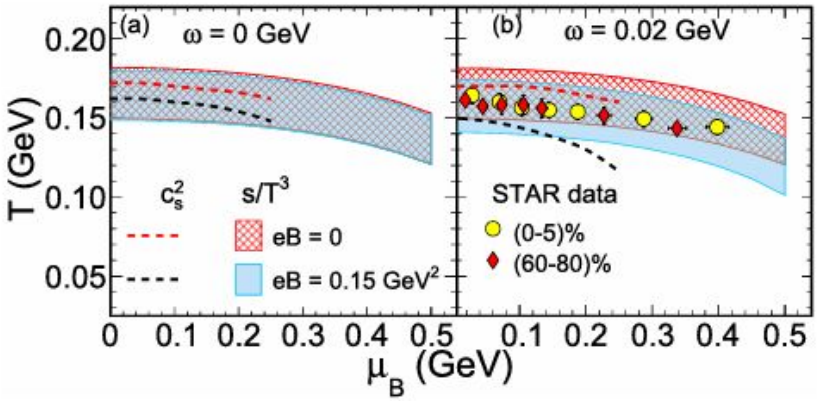

Fig. 2. QCD phase diagrams, T vs. μ_B for $eB = 0$ (red band or curve) and $eB = 0.15$ GeV^2 (blue band or curve) and (a) for $\omega = 0$ GeV and (b) for $\omega = 0.02$ GeV. The deconfinement transition zones depicted as (i) bands constrained by $s/T^3 = 4$ (lower edge) and 7 (upper edge), and (ii) curves obtained from the minima of c_s^2 vs. T as shown in Fig. 1.

In Fig. 2, we have also shown data points for chemical freezeout as extracted from experimental particle yields and ratios for two centrality classes, (0-5)% and (60-80)%. When such fitting analyses incorporate rotation and magnetic field as additional quasi-control parameters (μB , ω and eB, all dependent on collision energy and impact parameter or centrality), our phenomenological results may be better interpreted. The comparison might lead to not only T − μ freeze-out data serving as ‘thermometer’ and ‘baryometer’ but also possibly augment them with capabilities of ‘magnetometer’ and ‘anemometer’ to estimate the magnitudes of magnetic field and rotational motion prevalent in a HIC fireball. The degree of the relative influences of μ ,ω and eB might be constrained from other observable phenomena, for example measured polarization to independently constrain ω, etc.

Key findings, Conclusions

(and applications)

Simultaneous turning on of both eB and ω appears to significantly amplify the drop in T_C due to μ_B, by nearly 40 to 50 MeV

Accessing the HIC fireball properties by using this approach as a 'thermometer', 'baryometer', 'magnetometer' and 'anemometer'-like tool

The existing parameterization for chemical freeze-out data seems well-suited to be extended to include ω, eB along with T and μ_B

Implications: pronounced lowering of T_C may lead to a longer lifetime for the deconfined phase

This work may also shed some light on whether the two transition (chiral and deconfinement) temperatures stay locked in value or split as we turn on the various parameters to finite values.

HICs probe the phase space traversed by the early universe*

*along T-axis, near 0 net baryon density

The *quark-hadron transition region* that we have estimated in the phase diagram is where both

the **early universe** *passed through* and

heavy-ion collision fireball droplets *commute,* being created at particle colliders like RHIC, LHC, etc.

Could vortical fields and magnetic fields be present in the early universe too?

If yes (if they did exist in the microseconds old universe at the quark-hadron epoch), then their influence on the quark-hadron transition temperature could be important and should be taken into account

Observational constraints from the CMB may be obtained

Spatial inhomogeneity due to rotation and anisotropy from magnetic field may be important too

Evolution of the Universe: The Epochs

Modern Cosmology provides high-precision data to support this picture

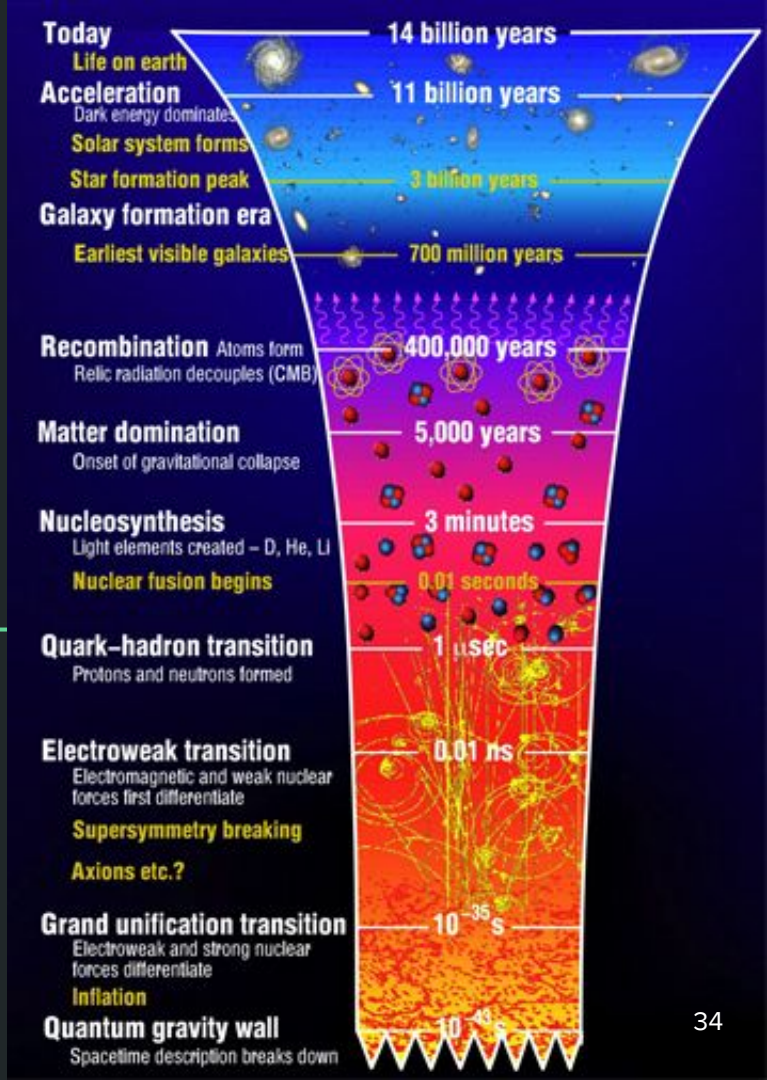

Vorticity and magnetic fields

Why can’t this be happening in the early universe?

Talks by Ruth, Tina and others explored this scenario too

1. In the quark-hadron epoch, the baryon-lepton fluid is predominantly composed of matter, not antimatter: due to prior baryogenesis
2. Baryons much heavier than leptons
3. Even quarks heavier than electrons

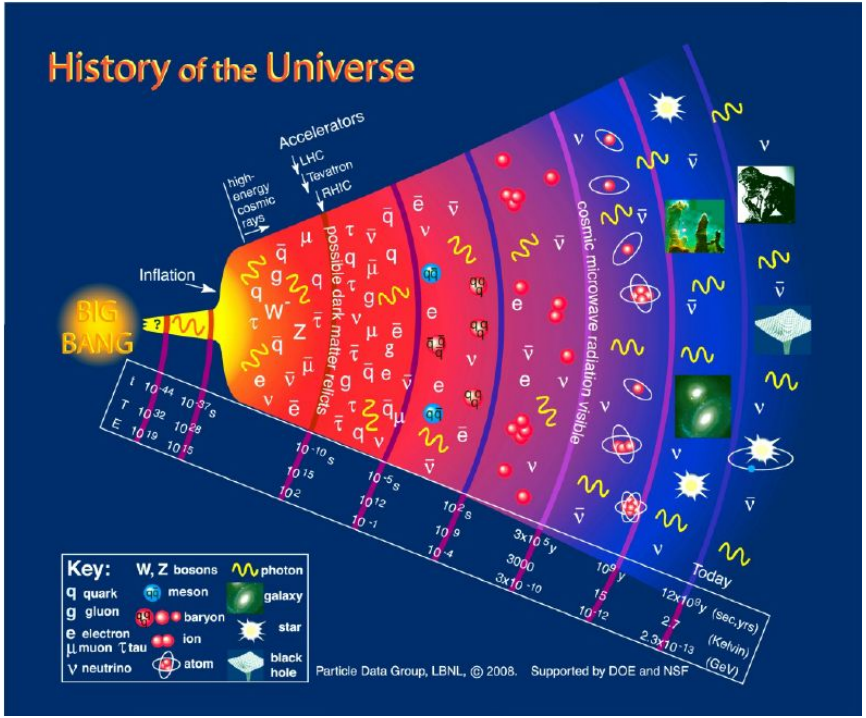

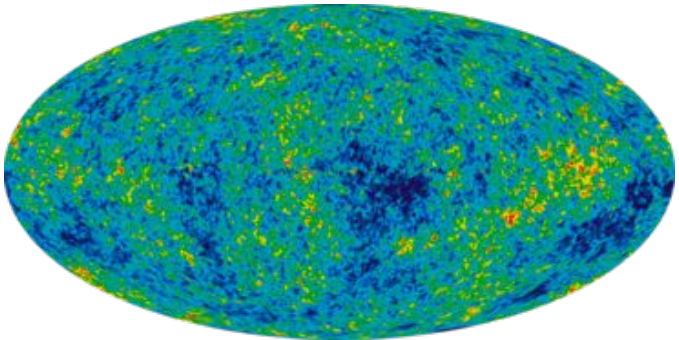

Primordial magnetogenesis:
proposed mechanism

1. Differential masses of the quarks (later baryons, mainly protons) and leptons could be responsible for a biased primordial distribution (stochastic, statistically isotropic) of local charged subatomic swirls

2. Spin hydrodynamic generation may be activated as demonstrated previously

3. Primordial magnetic fields take birth

4. The large scale magnetic fields found today may be seeded this way

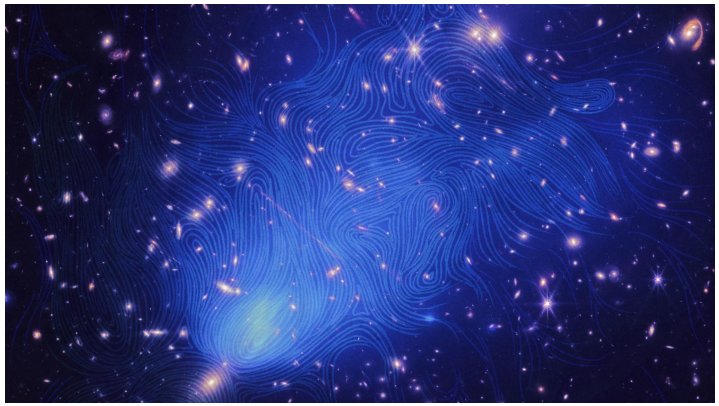

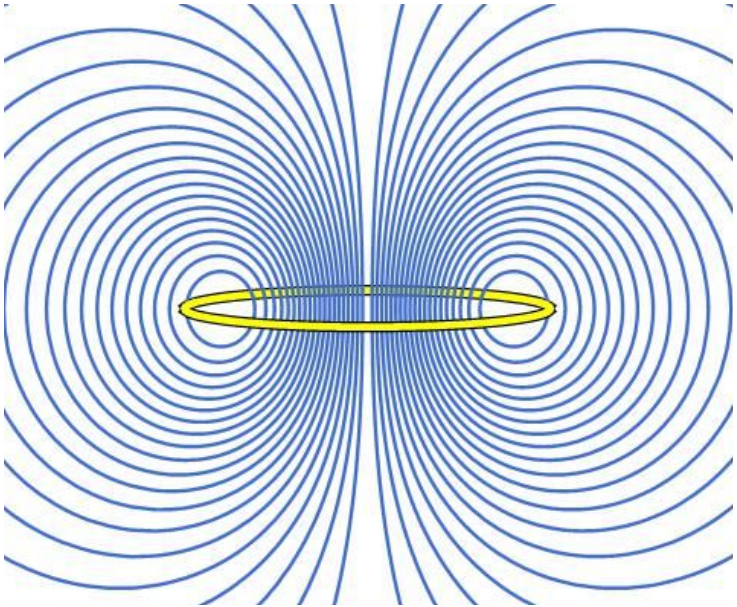

Conclusions

- We have an estimated quark-hadron deconfinement region in the QCD phase diagram that is augmented to incorporate the effects of parallel vorticity and magnetic field under ideal conditions
- This suggests in strong vortical and magnetic fields the confinement-deconfinement happens at somewhat cooler temperatures
- Heavy-ion phenomenological consequences should be important
- Experimentalists have partial control over proxies for the vorticity and magnetic field generated in HICs
- To connect with the problem of cosmological magnetogenesis and study the impact of the lowered transition temperature on the quark-hadron epoch and cosmological observables, more work is needed

Acknowledgements

Collaborators:

Dipanwita Dutta, Dipak Kumar Mishra

Heavy-ion collisions to early universe (quark-hadron epoch):

Can the theoretical framework be legitimately applied throughout?
If yes, what are the parameter ranges for each case?
Where does the model break down?

1. Homogeneity and Isotropy
2. Locally violated?
3. On what scales?
4. Dynamics and evolution to present times

References

https://atlas.cern/Discover/Physics

https://www.youtube.com/watch?v=m21016M8BgU&t=675s

https://cerncourier.com/a/going-with-the-flow/

https://phys.org/news/2011-05-cosmic-magnetic-fields.html

https://www.caltech.edu/about/news/caltech-astronomers-unveil-distant-protogalaxy-connected-cosmic-web-47459

https://www.americanscientist.org/article/the-cosmic-web

https://www.ctc.cam.ac.uk/outreach/origins/big_bang_three.php